This is an open access article published under an ACS AuthorChoice License, which permits copying and redistribution of the article or any adaptations for non-commercial purposes.

ACS OMEGA

http://pubs.acs.org/journal/acsodf

Article

Lignosulfonate Salt Tolerance and the Effect on Emulsion Stability

Jost Ruwoldt,* Juliette Planque, and Gisle Øye

Cite This: *ACS Omega* 2020, 5, 15007−15015

Read Online

ACCESS | Metrics & More | Article Recommendations

ABSTRACT: In this article, we adapted and compared methods to assess lignosulfonates for technical applications. Salt-induced agglomeration and precipitation were studied via mechanical separation and subsequent UV spectrometry. The effect of lignosulfonates on emulsion stability was investigated in two steps: measuring the amount of oil separated after centrifugation and subjecting the remaining emulsion to shear in a rheometer. To complement the results, interfacial tension (IFT) was measured by the spinning drop technique, and the droplet size distribution was determined via a laser scattering technique. The observed trends in lignosulfonate salt tolerance and emulsion stabilization efficiency were opposite; that is, samples with low salt tolerance generally exhibited better emulsion stabilization and vice versa. This tendency was further matched by the hydrophobic characteristic of the lignosulfonates. The droplet size distributions of lignosulfonate-stabilized emulsions were similar. The effect of lignosulfonates on IFT depended on the oil phase and sample concentration. As a general trend, the IFT was lower for lignosulfonates with low average molecular weights. It was concluded that the adapted techniques allowed for detailed assessment of lignosulfonates with respect to salt tolerance and emulsion stabilization. In addition, it was found that the suitability for these applications can to some extent be predicted by the analytical data.

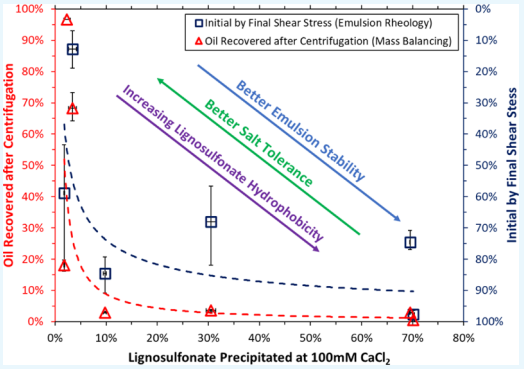

1. INTRODUCTION

Lignosulfonate, also referred to as sulfonated lignin, is a product of the wood pulping process. Initially considered as a waste material, refined lignosulfonate nowadays constitutes a viable alternative to synthetic chemicals in many applications.[1] Among others, it is used in dispersant formulations in concrete, for rheology control of drilling fluids and coal−water slurries, and as a germicide, a flotation agent, and an emulsion stabilizer.[2] In part because of its origin, lignosulfonate is a renewable chemical with low toxicity and good biodegradability.

With respect to the chemical composition and structure, lignosulfonate is similar to its precursor lignin. From a simplified viewpoint, lignin is a biopolymer that consists of monomers based on *p*-hydroxyphenyl, guaiacyl, and syringyl, which are randomly connected via ether or carbon−carbon bonds.[3,4] During sulfite pulping of lignocellulose biomass, the lignin polymer is degraded into smaller fragments and sulfonate groups are added, which account for the good solubility of lignosulfonates in water.[5,6] The chemical composition depends largely on the substrate, where softwood lignins and hardwood lignins can be distinguished. Softwood lignin is reported to consist almost entirely of guaiacylpropane units, whereas hardwood lignin contains both guaiacyl- and syringylpropane units.[4] The molecular weight distribution of hardwood lignin was found to be lower than that for softwood lignin.[7] Other factors that can influence the composition and characteristics of lignosulfonates are the reaction conditions during the sulfonation reaction, fractionation, and purification procedures, as well as chemical modifications.[4,7]

The behavior and characteristics of lignosulfonates in an aqueous solution depend strongly on factors such as salinity, pH, and lignosulfonate composition. Solubilized lignosulfonate molecules were reported to exhibit an ellipsoidal shape and self-associate on the flat edges into planar agglomerates.[8−10] Results from fluorescence spectrometry have suggested that lignosulfonate agglomeration can start at concentrations of 0.05−0.24 g/L.[11,12] Qian et al. further reported that increasing the temperature above ambient conditions can enhance hydrophobic interactions, which can cause lignosulfonate aggregation at elevated temperatures.[13] Besides, the presence of electrolytes can induce lignosulfonate precipitation, during which flocculates are formed, which have dimensions much larger than lignosulfonate aggregates. This destabilization was discovered to follow the Hofmeister series with the exception

Received: February 11, 2020
Accepted: June 3, 2020
Published: June 17, 2020

Downloaded via NORWEGIAN UNIV SCIENCE & TECHNOLOGY on January 5, 2021 at 10:34:20 (UTC).
See https://pubs.acs.org/sharingguidelines for options on how to legitimately share published articles.

© 2020 American Chemical Society

https://dx.doi.org/10.1021/acsomega.0c00616
ACS Omega 2020, 5, 15007−15015

of a few ions.[14] An increase in pH was reported to lead to size expansion by structural unfolding of both dissolved and aggregated lignosulfonates because of ionization of weakly hydrophilic groups.[12] The carboxylic groups were stated to ionize at about pH 3−4, whereas the phenolic groups may ionize at around pH 9−10.[12,15] Because lignosulfonate composition is precursor-dependent, hardwood and softwood lignosulfonates exhibit slight differences in solubility.[16] Softwood lignosulfonate was found to have a Hansen solubility parameter closer to water, as compared to hardwood lignosulfonate.

Adsorption of lignosulfonates on solid surfaces has been stated to follow the Langmuir isotherm.[17−20] The authors further found that straight-chain alcohols can enhance this adsorption.[21] In a different approach, the adsorption characteristics were investigated by building up multilayers of lignosulfonate and the cationic polymer, and it was concluded that hydrophobic interactions and cation−π interactions were dominant rather than electrostatic interactions.[22,23] Evidence for adsorption of lignosulfonates on the interface of binary oil−water mixtures is given by measurements of interfacial tension (IFT) or compression isotherms.[24,25]

The stabilization and destabilization of emulsions is a contemporary research topic with importance to, for example, food science or fuel production.[26−29] Lignosulfonate is a known stabilizer for oil-in-water emulsions.[24,30,31] The stabilization mechanism is most likely a combination of electrostatic repulsion, stearic hindrance, particle stabilization, and the formation of a semirigid interface layer.[31,32] Mixing of lignosulfonate and an anionic surfactant can yield improved surface activity,[33,34] but mixing with a cationic surfactant showed less potential.[35]

Lignosulfonate characterization generally measures properties such as elemental composition, the presence of functional groups, molecular weight distribution, and hydrophobicity.[36] The molecular weight is traditionally measured by size exclusion chromatography (SEC). An improvement to SEC was done by coupling with multiangle light scattering as the detection method.[7] Two-dimensional nuclear magnetic resonance spectroscopy has been extended to study the structural characterization of lignin and its derivatives.[37] Hydrophobic interaction chromatography (HIC) is a technique that uses lignosulfonate adsorption on a stationary phase and subsequent desorption with solvents of different polarities for fractionation.[38] As the elution time progresses, the eluent ratio of alcohol to water is increased stepwise, each producing a new eluent peak that can be used to quantify the hydrophobicity of the sample.

Recent developments have enabled better understanding of lignosulfonate properties and behavior in aqueous solutions. However, a lack of systematic studies was stated, which could establish a connection between these properties and practical applications.[4] In addition, industrial efforts have yielded more specialized lignosulfonate products, which are reflected, for example, by a diversification of lignosulfonate hydrophobicity. In this article, we therefore adapted and compared methods to evaluate lignosulfonates, where the focus is on salt tolerance and emulsion stability. In addition, the effect of lignosulfonate on emulsion characteristics and IFT were studied. The goal was to establish templates for testing procedures and comparison, which would benefit lignosulfonate utilization in technical applications.

2. EXPERIMENTAL SECTION

2.1. Materials. Xylene isomer blend (≥97%, HPLC-grade) was purchased from VWR, Norway. Mineral oil was provided as Exxsol D60 from ExxonMobil Corporation. All water used in this study was purified via a Millipore water purification system (resistivity: 18.2 MΩ). Salts were obtained as sodium chloride (≥99.5%), calcium chloride dihydrate (≥99%), magnesium chloride hexahydrate (≥99.0%, BioXtra), and aluminum chloride hexahydrate (≥97%) from Sigma-Aldrich, Norway.

2.1.1. Lignosulfonate Samples. All samples used in this study are commercial sodium lignosulfonates that were purified and analyzed by Borregaard AS. Some of these lignosulfonates may have undergone novel fractionation or chemical modification processes, which are proprietary to Borregaard AS. All lignosulfonates are therefore treated via a black box approach; however, it should be noted that the sample characteristics are more diverse than for traditional lignosulfonates. The number-average molecular weight (M_n) is listed in Table 1, which was determined by gel permeation chromatography.[7]

Table 1. Number-Average Molecular Weight of Lignosulfonate Samples

	LS-1	LS-2	LS-3	LS-4	LS-5	LS-6	LS-7
M_n (g/mol)	2700	3500	2700	2800	3200	1800	4000

All samples were also provided with data from HIC,[38] which are given in Table 2. HIC peak distributions were converted into a single numerical value via eq 1, the relative hydrophobicity I_{hyd}. This was done to enable a better overview and comparison between different samples. The relative hydrophobicity, I_{hyd}, is a dimensionless number between 0 and 1, where low values correspond to less and high values correspond to more hydrophobic characteristic of the sample. It is calculated from the area of the ith peak p_i using a peak number i and a maximum peak number n.

Table 2. HIC Peak Distribution and Relative Hydrophobicity[a]

peak area	LS-1	LS-2	LS-3	LS-4	LS-5	LS-6	LS-7
peak 1 (vol %)	69	48	43	28	20	12	22
peak 2 (vol %)	18	22	22	11	12	13	7
peak 3 (vol %)	11	25	31	25	32	32	13
peak 4 (vol %)	<2	5	4	30	34	35	13
peak 5 (vol %)	<2	<2	<2	6	<2	8	45
sum (vol %)	98	100	100	100	100	100	100
relative hydrophobicity	0.1	0.22	0.24	0.44	0.47	0.54	0.63

[a]The nomenclature of lignosulfonate samples was based on the order of hydrophobicity, that is, increasing sample index (LS-1, LS-2, etc.) also implies increasing relative hydrophobicity.

$$I_{hyd} = \frac{\sum_i^n \left(\frac{p_i}{\sum_i^n p_i} \cdot i \right) - 1}{n - 1} \quad (1)$$

2.2. Sample Preparation. The samples were prepared by adding stock solutions of first lignosulfonate and then water and salt to a volumetric flask. The salt is always added after diluting the lignosulfonate close to the target concentration,

https://dx.doi.org/10.1021/acsomega.0c00616
ACS Omega 2020, 5, 15007−15015

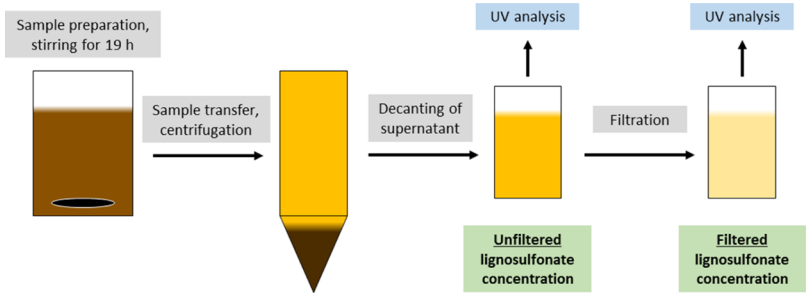

Figure 1. Schematic for measuring salt tolerance of lignosulfonates.

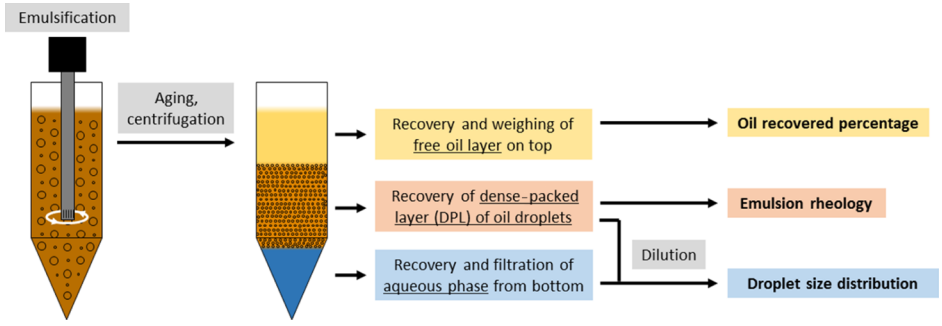

Figure 2. Schematic for measuring the lignosulfonate effect on emulsion stability and characteristics.

which is done to prevent the formation of irreversible agglomerates. After preparation, the samples were gently shaken by hand and sonicated for 10 min. IFT was measured within 3 days after solution making because no influence of time for this type of measurement was found. Lignosulfonate solutions for salt tolerance experiments were aged for exactly 19 h before processing, as the aging time could have an influence. Solutions were not pH-adjusted, as this would impact the ionic strength of the solution. All experiments were conducted at ambient conditions with a temperature of 22 ± 1 °C.

2.3. Salt Tolerance of Lignosulfonates. To test the salt tolerance of lignosulfonates, the procedure depicted in Figure 1 was developed. In this procedure, the sample undergoes mechanical separation after the equilibration period. At first, centrifugation at 8000 rpm is done for 5 min in an Eppendorf 5810 centrifuge. The supernatant is decanted for UV analysis. The bottom sludge was dried in an oven and weighed for mass balancing, but this was solely used for verification of UV measurements because the bottom sludge also contained varying amounts of aqueous phase with dissolved components. Part of the decanted supernatant is also filtrated through a 0.2 μm polypropylene syringe filter and collected for UV analysis.

In UV analysis, both the filtered and the unfiltered phase were further diluted by a factor of 50−100 in water. The dilute solution was analyzed in a Shimadzu UV-2401PC UV/vis spectrometer, where the absorbance at 280 nm was used for quantification. A calibration line was established by measuring defined concentrations of lignosulfonate. The absorbance was at all times linearly proportional to the sample concentration within the established limits, which also indicated that no lignosulfonate agglomeration occurred in the analyte. Two to four measurements were made per sample composition and the deviation from the mean was no more than 1%.

A decrease of lignosulfonate concentration after centrifugation indicated lignosulfonate precipitation. Centrifuging longer and at higher speeds yielded the same amount of precipitate within the established experimental error. If the concentration decreased after filtration, this was associated with lignosulfonate agglomerate growth because the agglomerates became large enough to be retained by the filter. High salt tolerance was associated with lignosulfonate samples, which required high amounts of salt to exhibit precipitation or agglomeration.

2.4. IFT Measurements. IFT was measured with a spinning drop video tensiometer SVT20 from DataPhysics Instruments GmbH, Germany. A 622/400-HT Fast Exchange Capillary was filled with the aqueous solution, and the oil phase was injected via a syringe, ideally consisting of one or two drops. The capillary was sealed, inserted into the tensiometer, and rotated at 8500−11,000 rpm during the experiment. Measurements were made via the SVTS 20 IFT software, which monitored the elliptical profile of a single drop to calculate the IFT according to the method of Cayias, Schlechter, and Wade. Because lignosulfonate adsorption on the oil−water interphase is a kinetic process, the IFT was monitored over time, and equilibrium was assumed if the instrument did not record a change in IFT for at least 30 min. This condition was usually fulfilled at 2.5 h or later. Once equilibrated, the calibration procedure of the instrument was repeated to yield up to four measurements per experiment, each with a new calibration. This procedure was adapted to provide a better statistical significance to the calibration procedure, which consisted of measuring the number of pixels during horizontal translation of the camera. Two to four experiments were made for each sample, depending on reproducibility.

2.5. Lignosulfonate Effect on Emulsion Stability and Characteristics. *2.5.1. Emulsification.* All emulsions were prepared by high-speed mixing at 18,000 rpm for 2 min with an Ultra Turrax T 25 fitted with a 18 mm head from IKA-Werke GmbH & Co. KG, Germany. Emulsions were prepared in 40 mL glass (quiescent emulsion stability) or 45 mL Eppendorf centrifugation vials (centrifuged emulsions). The

https://dx.doi.org/10.1021/acsomega.0c00616
ACS Omega 2020, 5, 15007−15015

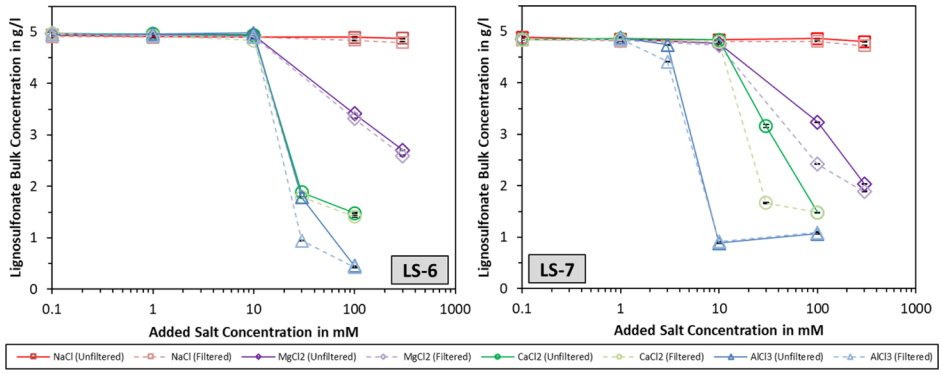

Figure 3. Average concentration of bulk lignosulfonate in aqueous solution with respect to the added salt concentration for LS-6 (left) and LS-7 (right). Error bars mark the maximum and minimum of each data point.

aqueous phase contained 0.1 wt % NaCl at all times as a background electrolyte.

2.5.2. Quiescent Emulsion Stability. The effect of lignosulfonate concentration on emulsion stability under quiescent conditions was studied on 50/50 (v/v) emulsions of xylene in aqueous solution (15 mL each). After emulsification, the vial was sealed at the top, and images were taken at defined time intervals.

2.5.3. Stability and Characteristics of Centrifuged Emulsions. A schematic of the procedure for measuring emulsion stability and characteristics is given in Figure 2. At first, 20 mL of mineral oil (Exxsol D60) was emulsified in 13.3 mL of aqueous solution with 5 g/L of lignosulfonate, yielding a ratio of 60/40 (v/v) oil to aqueous phase. The emulsions were aged overnight and centrifuged the next day at 5000 rpm for 20 min. The free oil phase at the top of each vial was carefully removed, collected, and weighed. This weight was divided by the amount of emulsified oil to obtain the recovered oil percentage. The aqueous phase at the vial bottom was also removed and collected, which left a dense packed layer (DPL) of oil droplets in the centrifugation vial. Prior to sampling, this DPL was gently stirred to provide a homogeneous sample while not promoting coalescence.

Emulsion rheology was measured in an Anton Paar Physica 301 rheometer. A representative sample of the DPL oil droplets (no dilution) was loaded into the cone and plate geometry (2° cone inclination, 4 cm cone diameter, and 0.17 mm gap size). The surfaces of the geometry had been sandblasted to provide additional roughness. The measurement procedure started with 2 min of quiescent rest, followed by a frequency sweep from 0.1 to 10 Hz at a strain of 0.1%, which was further followed by a strain sweep from 0.01 to 100% at 1 Hz. Shearing at constant 10 s^{-1} was subsequently done for 2 min to provide consistent preshearing conditions, followed by a shear rate sweep from 0.1 to 100 s^{-1} repeated in reverse order from 100 to 0.1 s^{-1}.

For droplet size measurements, the aqueous phase was filtrated through a 0.2 μm polypropylene syringe filter. This was done to remove the remaining droplets or aggregates, which could otherwise obscure the measurement. Part of the filtrate was used to dilute a representative sample of the DPL, yielding an initial dilution ratio of 10 or higher by volume. Laser diffraction technique was used to determine the droplet size distribution using a Mastersizer 3000 fitted with Hydro SV sample unit from Malvern Instruments Ltd, UK. Stirring speed and data acquisition had been optimized to minimize effects such as droplet coalescence, breakup, or creaming, which could otherwise skew the experimental outcome. The sample cell was preloaded with an aqueous filtrate, and the diluted droplets were slowly injected under constant stirring at 1500 rpm. Sample dosing was done to maintain a laser obscurity within the 8−16% range to minimize the possibility of multiple scattering. Measurements were performed with both red laser (633 nm) and blue light source (470 nm) in 10 s intervals for a duration of 5 min. The droplet size distribution was extracted from the data measured right after reaching maximum obscurity.

3. RESULTS AND DISCUSSION

3.1. Lignosulfonate Agglomeration and Salt Tolerance. The outcome of salt tolerance experiments is exemplarily plotted in Figure 3 for the two most hydrophobic lignosulfonates, LS-6 and LS-7. Reproducibility of individual measurements was generally good. At low salt concentrations, the lignosulfonate bulk concentration remains constant at 5 g/L. At higher salinities, the electrical double layer between the lignosulfonate molecules can be highly compressed, which would facilitate intermolecular association, yielding agglomeration and precipitation.[39] This effect is visible at $AlCl_3$ concentrations above 1 mM (LS-7) or 10 mM (LS-6), where the bulk concentration started decreasing as a result of salting out. Lignosulfonate precipitation is indicated by a concentration decrease after centrifugation (unfiltered concentration). Both onset concentration and severity, that is, the amount of lignosulfonate lost from the bulk solution, were in line with the Hofmeister series. $AlCl_3$ showed the largest potential for salting out, followed by $CaCl_2$, $MgCl_2$, and at last NaCl. In addition, results often mirrored the Schulze Hardy rule, which states that the critical coagulation concentration of colloidal suspensions is inversely proportional to the sixth power of the charge number of the counterion. These results are in agreement with the findings of Myrvold.[4,14]

As can also be seen in Figure 3, the lignosulfonate concentration after filtration is always below the unfiltered sample. This difference is more pronounced in regions where a considerable amount of lignosulfonate has precipitated. A fraction of the aggregates therefore appears to be large enough to be retained by the 0.2 μm filter but not large enough to be removed during centrifugation. Moreover, the difference between filtered and unfiltered concentration could increase right before the precipitation onset. This would indicate that the growth of lignosulfonate agglomerates may precede large-scale precipitation.

https://dx.doi.org/10.1021/acsomega.0c00616
ACS Omega 2020, 5, 15007−15015

Two special cases were found, in which LS-2 and LS-3 showed lignosulfonate precipitation at an $AlCl_3$ concentration of 10 mM, but at higher $AlCl_3$ concentrations, the precipitation would become less or even diminish completely. An explanation for this behavior would be that charge reversal is occurring around the lignosulfonate molecules, which promotes salting-in behavior at increased $AlCl_3$ concentrations. Similar effects were observed, for example, for the complexation of cationic surfactants with lignosulfonates.[35]

The unfiltered lignosulfonate concentration can furthermore be used to compute the amount of precipitated lignosulfonate LS_p, as stated in eq 2. The underlying assumption is that all lignosulfonate removed during centrifugation constitutes the precipitate. The aqueous-phase concentration, c_{aq}, of dissolved lignosulfonate was assumed to be homogeneous, so removing part of the aqueous phase with the precipitate sludge did not affect the calculation. The total or initial lignosulfonate concentration is denoted by c_0.

$$LS_p = 1 - \frac{c_{aq}}{c_0} \tag{2}$$

A comparison of different lignosulfonate samples for salting out with $CaCl_2$ is shown in Figure 4. The least hydrophobic

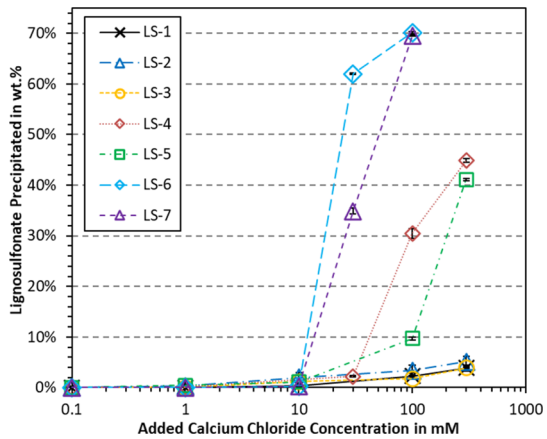

Figure 4. Average percentage of lignosulfonate precipitated because of $CaCl_2$ addition to the aqueous solutions of 5 g/L of lignosulfonate. Error bars mark the maximum and minimum of each data point.

lignosulfonates LS-1, LS-2, and LS-3 exhibit low precipitation percentages even at 300 mM $CaCl_2$. The samples LS-4 and LS-5 showed 10−30 wt % precipitation mass at 100 mM $CaCl_2$, and the most hydrophobic lignosulfonates LS-6 and LS-7 show an even earlier precipitation onset. Precipitation onset and the amount of precipitate are aggravated with increasing hydrophobicity. The order of relative hydrophobicity is not followed exactly, as the samples may be switched by one position compared to the order of salt tolerance. Still, the overall trend is consistent.

The maximum percentage of lignosulfonate precipitated was generally within a range of 50−90 wt % for $AlCl_3$, which exhibited the largest salting out tendency. Even at high amounts of salt, the lignosulfonate bulk concentration was never zero. This observation could be the result of charge reversal and salting-in phenomena, as discussed above. In addition, the lignosulfonates were in all cases technical samples, which are polydisperse. As a consequence, certain fractions within the sample might be more salt tolerant than others, which could prevent a total salting out of the lignosulfonates.

3.2. Lignosulfonate Effect on IFT. IFT is of interest when considering the application of lignosulfonates for emulsification and emulsion stabilization because low IFT can promote emulsification. Surface tension measurements have been used by many authors to characterize lignosulfonates and their interactions with surfactants,[12,21,34,35,40] but the lignosulfonate effect on IFT has been limited to petroleum technology.[24,41]

The effect of concentration on the IFT of four lignosulfonates is shown in Figure 5. In this linear-logarithmic

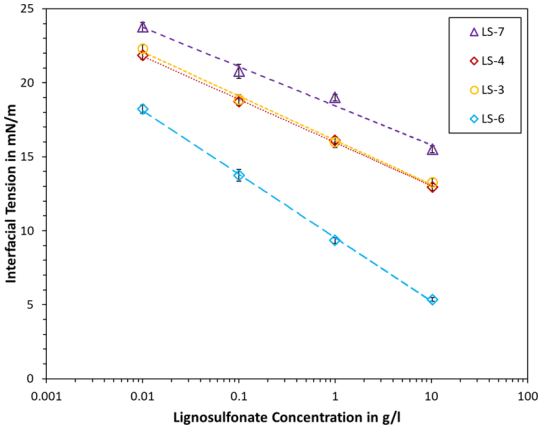

Figure 5. Effect of lignosulfonate concentration on the IFT of the xylene−brine (3.5 wt % NaCl in water) interface. Each data point is the average of at least two experimental runs (three to four measurements per run) with the corresponding standard deviation.

plot, all samples closely follow a straight line, which is in agreement with the results published by Syahputra et al.[41] Some deviation from the straight line occurred because of data scattering, but all data points are within 2σ of the regression line. A high-salinity environment (3.5 wt % NaCl) was chosen to probe if lignosulfonate aggregation might influence IFT, which would show as a deviation from the straight-line progression. This was not the case within the tested concentration range of 0.01−10 g/L. Moreover, it can be said that the lignosulfonate behavior resembled that of regular ionic or nonionic surfactants for the chosen settings.

The results from Figure 5 can further be used for calculations via Gibbs adsorption isotherm, for which the slope of each graph is determined. The surface excess per unit area Γ is calculated via eq 3 using temperature T, ideal gas constant R, IFT γ, and lignosulfonate concentration c_{LS}. This equation is also valid for strong surfactant electrolytes, as long as a high concentration of an indifferent electrolyte is given, such as NaCl.

$$\Gamma = -\frac{1}{RT}\left(\frac{\partial \gamma}{\partial \ln c_{LS}}\right) \tag{3}$$

The surface excess per unit area Γ was further converted from mol/m^2 to mg/m^2 via the number-average molecular weight M_n of lignosulfonates. In addition, the area per molecule A_m can be computed as stated in eq 4, where N_{av} is Avogadro's constant.[42]

https://dx.doi.org/10.1021/acsomega.0c00616
ACS Omega 2020, 5, 15007−15015

$$A_m = \frac{1}{\Gamma N_{av}} \quad (4)$$

The final values are listed in Table 3. The surface excess per unit area was in the range of 1−2 mg/m^2 for all tested samples.

Table 3. Surface Excess and Area per Molecule Calculated via Gibbs Isotherm

lignosulfonate sample	surface excess per unit area (mol/m^2)	surface excess per unit area (mg/m^2)	area per molecule (Å^2)
LS-3	5.25 × 10^{-7}	1.42	316
LS-4	5.13 × 10^{-7}	1.44	324
LS-6	7.50 × 10^{-7}	1.35	221
LS-7	4.64 × 10^{-7}	1.86	358

The area per molecule follows the exact same order as the average molecular weight, which would rank LS-6 < LS-3 < LS-4 < LS-7 from lowest to highest. Other authors determined a lignosulfonate spheroid thickness of 1−1.4 nm by anomalous small-angle scattering.[9] Assuming a circular shape, the area per molecule of Table 3 would result in a diameter of 1.7−2.1 nm, which is within the same order of magnitude. The two techniques therefore appear to be in close agreement, and differences could be explained by geometrical simplifications or the use of dissimilar lignosulfonate samples.

No correspondence between hydrophobicity and effect on IFT was found. The average molecular weight was plotted against the lignosulfonate effect on IFT in Figure 6. As can be

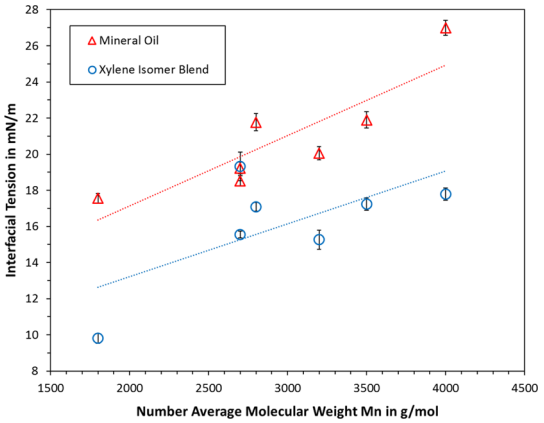

Figure 6. IFT in dependence of number-average molecular weight of different lignosulfonates at a concentration of 5 g/L in aqueous solution with 0.1 wt % NaCl. Each data point is the average of at least two experimental runs (three to four measurements per run) with the corresponding standard deviation. The dotted lines are linear regression lines.

seen, a general trend is that lignosulfonates with lower molecular weight also decrease the IFT more. This makes sense when considering that experiments were done at a constant mass concentration. IFT is also a function of molar concentration, which will then be higher at lower average molecular weight. The individual data points in Figure 6 exhibit scattering with up to 5 mN/m deviation from the fitted regression line. Two factors may contribute to this scattering, which can both be attributed to sample polydispersity. On the one hand, the lignosulfonate samples may be chemically different, for example, by containing different ratios of functional groups. On the other hand, the molecular weight is only an average value that may not fully represent the molecular weight distribution of the entire sample. Still, from a technical point of view, it can be concluded that low-molecular-weight lignosulfonates are more suited for reducing the IFT of oil−water systems.

3.3. Lignosulfonate Effect on Emulsion Stability and Characteristics. Two different approaches were made to test the ability of lignosulfonates to stabilize oil-in-water emulsions. The first approach consisted of emulsifying oil at varying lignosulfonate concentrations to observe coalescence during quiescent storage. Emulsions stabilized by 0.1 g/L of lignosulfonate in aqueous solution are displayed in Figure 7.

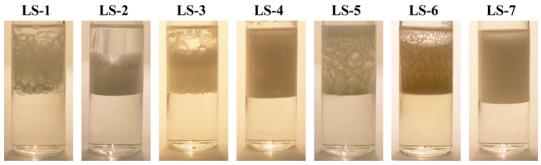

Figure 7. Emulsions of 50/50 (v/v) xylene in water stabilized by 0.1 g/L of lignosulfonate in aqueous solution with 0.1 wt % NaCl. Images were taken 1 d after emulsification.

Each frame shows the separated aqueous phase at the lower half, a creamed emulsified phase in the upper half, and sometimes a free oil layer at the top. Random tests were conducted using microscopy and dilution in larger volumes, which confirmed that the emulsions were oil-in-water in each case.

As can also be seen in Figure 7, the emulsions with low hydrophobicity lignosulfonates (LS-1 to LS-3) display larger droplet sizes and a free oil layer, both of which are the result of droplet coalescence. Similar observations were also made for more hydrophobic lignosulfonates (LS-4 to LS-7), but coalescence is generally less pronounced. At 1 g/L of lignosulfonate in the aqueous phase, no separation was observed even after 10 d of quiescent storage except for LS-1. At 0.03 of g/L lignosulfonate in water, complete separation was observed for LS-1, LS-2, LS-3, and LS-5 within 1 h, while LS-6 required longer than 1 h, and LS-4 and LS-7 still exhibited a portion of emulsified oil even after 10 d.

Under quiescent storage, coalescence could yield larger droplets that did not merge with the free oil layer at the top, as shown in Figure 7. The height of the free oil layer could therefore not be used for quantification, and a centrifugation procedure was hence developed. After centrifugation, the free oil layer on top was collected and weighed, which provided the amount of oil recovered in percentage of the total oil that had been emulsified. The results are plotted in Figure 8. In this testing procedure, the samples LS-1 and LS-2 showed comparably unstable emulsions, where more than 50 wt % of the input oil was recovered. The more hydrophobic lignosulfonates (LS-4 to LS-7) all yielded stable emulsions with less than 4 wt % oil recovered. The best emulsion stability in this test was for LS-6 at 0.5 wt % oil recovered.

To further probe the emulsion stability, rheometric experiments were conducted. Frequency and amplitude sweep showed viscoelastic behavior for all emulsions and a limit of approximately 1% strain for the linear viscoelastic region. Shear rate sweeps are plotted in Figure 9. As can be seen, the emulsions exhibit thixotropic and shear-thickening behavior. A general trend is that samples with lower emulsion stability also

https://dx.doi.org/10.1021/acsomega.0c00616
ACS Omega 2020, 5, 15007−15015

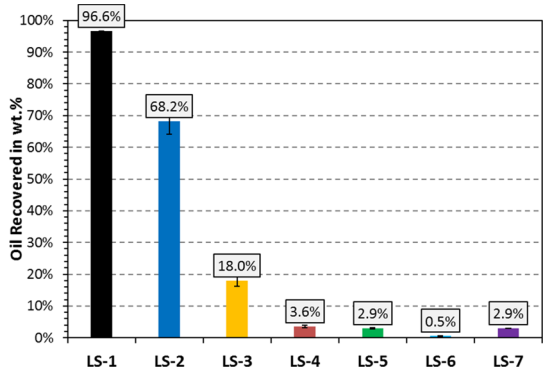

Figure 8. Emulsion stability measured in percentage of oil recovered after centrifugation. Emulsions of 60/40 (v/v) mineral oil in water were stabilized by 5 g/L of lignosulfonate in aqueous solution with 0.1 wt % NaCl. The data were averaged over three measurements with error bars, indicating the maximum and minimum value.

show lower shear stress, which can be the result of droplet coalescence during preshearing. However, the shear stress can also depend on factors such as the aqueous volume fraction.[43] A better approach to quantify shear tolerance is therefore to consider the shear hysteresis. This hysteresis is visible for all samples, where upon increasing the shear rate, the shear stress becomes larger than that during the subsequent sweep with decreasing shear rate. The ratios of shear stresses at 0.1 s^{-1} are also plotted in Figure 9, which represent the decrease from the initial to final value during the shear rate sweep. Higher shear stress ratios indicate lower reduction in the rheological response of the emulsion, which further implies better stability and therefore shear tolerance. Data scattering is pronounced in Figure 9, which would, for example, render the difference between LS-3, LS-4, and LS-5 uncertain. However, the same trend as the oil recovered in Figure 8 was observed, which corroborates the results of Figure 9. Lower hydrophobicity lignosulfonates (LS-2 and LS-3) yielded lower emulsion stability than more hydrophobic lignosulfonates. Analogously, LS-6 exhibited the best shear tolerance, followed by LS-5 and further by LS-7 and LS-4.

Comparing the different lignosulfonates, the stability of mineral oil in water emulsion directly follows the order of hydrophobicity. An exception is made by LS-7. This poorer performance could be explained by higher IFT (see Figure 6), which in turn could be due to the high molecular weight of LS-7. On the other hand, xylene-in-water emulsions (see Figure 7) documented a better emulsion stability for LS-7. Considering that the lignosulfonate effect on IFT also depended on oil phase, it is evident that the oil-phase composition may influence the interfacial activity of lignosulfonates. Still, the overall conclusion is that lignosulfonates with high hydrophobicity are the most suitable for emulsion stabilization.

Droplet size distributions after centrifugation were measured by a laser scattering technique. The results are plotted in Figure 10. All lignosulfonates yielded similar size distributions,

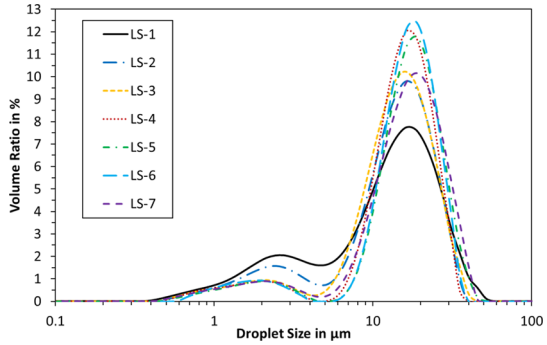

Figure 10. Droplet size distribution measured by the laser scattering technique of emulsion after centrifugation. Each graph represents the average of three measurements.

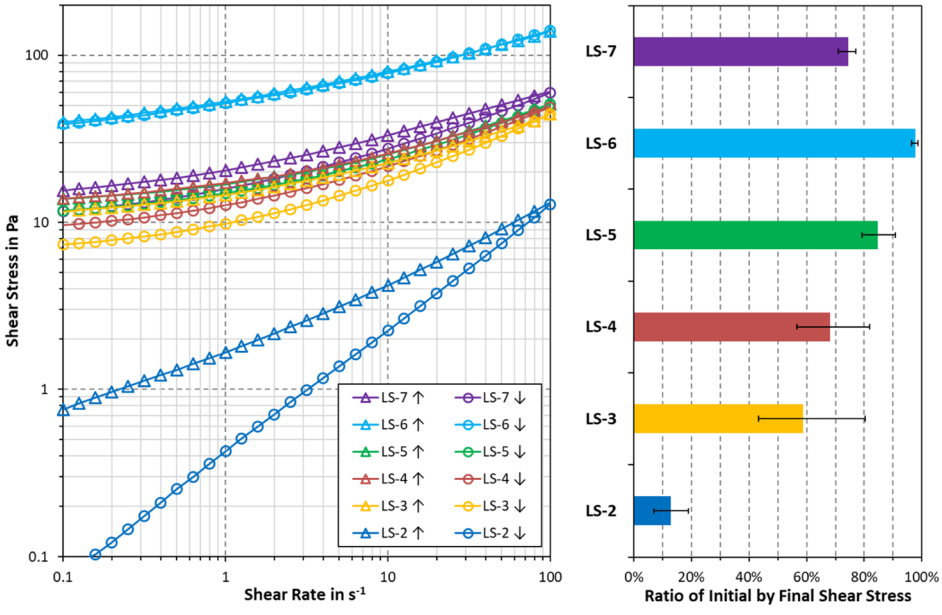

Figure 9. Emulsion shear tolerance studied by shear sweep (left) as well as the ratio of initial and final yield stress at 0.1 s^{-1} (right) of DPL emulsions retrieved after centrifugation. Emulsions of 60/40 (v/v) mineral oil in water were stabilized by 5 g/L of lignosulfonate in aqueous solution with 0.1 wt % NaCl. Upward arrows ↑ indicate progressive increases in shear rate, whereas downward arrows ↓ indicate a progressive decrease. The data were averaged over three measurements with error bars, indicating the maximum and minimum value.

https://dx.doi.org/10.1021/acsomega.0c00616
ACS Omega 2020, 5, 15007−15015

which were bimodal and had the largest peak with a maximum between 10 and 20 μm. The peak maximum for each sample was reproducible within ±5 μm and the Sauter diameter was reproducible within ±1 μm. Scattering could be the result of the material lost during the dilution process, but no effect of dilution ratio was noted as long as the laser obscurity remained sufficiently low.

The similarity in droplet size distribution is likely due to a similar effect on IFT, as all samples measured values between 17 and 27 mN/m for the chosen settings. The two lignosulfonates with the lowest emulsion stability (LS-1 and LS-2) exhibited a larger secondary peak around the local maximum of 1−2 μm. This observation stems from the fact that LS-1 and LS-2 had the highest oil recovery percentages, as shown in Figure 8. Coalescence of larger droplets is favored over smaller droplets, which will shift the droplet size distribution toward smaller droplets during centrifugation. In contrast, the droplet size distributions of more stable emulsions tend to be narrower. In comparison to the results published by other authors, the droplet size distributions of Figure 10 are approximately one magnitude larger.[44] This is likely due to a difference in emulsion preparation and the fact that the emulsions in this study were centrifuged before measurement.

4. SUMMARY AND CONCLUSIONS

In this study, methods were adapted to investigate the salt tolerance of sodium lignosulfonates and their emulsion stabilization efficiency. In addition, droplet size distributions and lignosulfonate effect on IFT were studied. The results were furthermore discussed with respect to the analytical data provided with the samples, more specifically hydrophobicity and average molecular weight.

The trend in salt tolerance among lignosulfonate samples was opposite to the emulsion stabilization efficiency; that is, samples with lower salt tolerance yielded on average more stable emulsions and vice versa. This observation was further matched by the hydrophobic characteristic of the lignosulfonates, where high hydrophobicity facilitated better emulsion stabilization and low hydrophobicity encompassed better salt tolerance. Recent developments have diversified the hydrophobicity scale of lignosulfonates, which is corroborated by the availability of more specialized products.

With respect to the type of added salt, lignosulfonate salting-out followed both the Hofmeister series and the Schulze−Hardy rule. Lignosulfonate-stabilized emulsions showed overall similar droplet size distributions. The IFT decreased as a logarithmic function when increasing lignosulfonate concentration from 0.01 to 10 g/L. A general tendency was found in that lignosulfonates with lower average molecular weight also induced larger decreases in IFT.

In conclusion, the adapted methods allowed more detailed assessment of lignosulfonate emulsion stabilization and salting-out phenomena. In addition, it was found that the suitability of sodium lignosulfonates for technical applications can be predicted by the analytical data to some extent.

AUTHOR INFORMATION

Corresponding Author

Jost Ruwoldt − *Ugelstad Laboratory, Department of Chemical Engineering, Norwegian University of Science and Technology (NTNU), 7491 Trondheim, Norway;* orcid.org/0000-0002-0583-224X; Email: jostru.chemeng@gmail.com

Authors

Juliette Planque − *École Nationale Supérieure de Chimie de Mulhouse (ENSCMu), University of Upper Alsace (UHA), 68200 Mulhouse, France*

Gisle Øye − *Ugelstad Laboratory, Department of Chemical Engineering, Norwegian University of Science and Technology (NTNU), 7491 Trondheim, Norway*

Complete contact information is available at: https://pubs.acs.org/10.1021/acsomega.0c00616

Notes

The authors declare no competing financial interest.

ACKNOWLEDGMENTS

This work was carried out as part of the project Ligno2G: second-generation performance chemicals from lignin, grant number 269570. The authors gratefully acknowledge the financial support from the Norwegian Research Council and Borregaard AS. The authors would further like to thank Dr. Sebastien Simon for helpful discussions.

REFERENCES

(1) Lauten, R. A.; Myrvold, B. O.; Gundersen, S. A. New developments in the commercial utilization of lignosulfonates. *Surfactants from Renewable Resources*; John Wiley & Sons, 2010; pp 269−283.

(2) Xu, C.; Ferdosian, F. Utilization of Lignosulfonate as Dispersants or Surfactants. In *Conversion of Lignin into Bio-Based Chemicals and Materials*; Xu, C., Ferdosian, F., Eds.; Springer-Verlag: Berlin, Heidelberg, 2017; pp 81−90.

(3) Rencoret, J.; Gutiérrez, A.; Nieto, L.; Jiménez-Barbero, J.; Faulds, C. B.; Kim, H.; Ralph, J.; Martínez, Á. T.; del Río, J. C. Lignin Composition and Structure in Young versus Adult Eucalyptus globulus Plants. *Plant Physiol.* **2011**, *155*, 667−682.

(4) Myrvold, B. O. Differences in solubility parameters and susceptibility to salting-out between softwood and hardwood lignosulfonates. *Holzforschung* **2016**, *70*, 1015−1021.

(5) Madad, N.; Chebil, L.; Sanchez, C.; Ghoul, M. Effect of molecular weight distribution on chemical, structural and physicochemical properties of sodium lignosulfonates. *Rasayan J. Chem.* **2011**, *4*, 189−202.

(6) Rojas, O.; Salager, J.-L. Surface activity of bagasse lignin derivatives found in the spent liquor of soda pulping plants. *Tappi J.* **1994**, *77*, 169−174.

(7) Braaten, S. M.; Christensen, B. E.; Fredheim, G. E. Comparison of Molecular Weight and Molecular Weight Distributions of Softwood and Hardwood Lignosulfonates. *J. Wood Chem. Technol.* **2003**, *23*, 197−215.

(8) Vainio, U.; Lauten, R. A.; Serimaa, R. Small-Angle X-ray Scattering and Rheological Characterization of Aqueous Lignosulfonate Solutions. *Langmuir* **2008**, *24*, 7735−7743.

(9) Vainio, U.; Lauten, R. A.; Haas, S.; Svedström, K.; Veiga, L. S. I.; Hoell, A.; Serimaa, R. Distribution of Counterions around Lignosulfonate Macromolecules in Different Polar Solvent Mixtures. *Langmuir* **2012**, *28*, 2465−2475.

(10) Myrvold, B. O. A new model for the structure of lignosulphonates: Part 1. Behaviour in dilute solutions. *Ind. Crops Prod.* **2008**, *27*, 214−219.

(11) Li, B.; Ouyang, X. P. In Structure and properties of Lignosulfonate with different molecular weight isolated by gel column chromatography. *Advanced Materials Research*; Trans Tech Publications Ltd., 2012; pp 2024−2030.

(12) Yan, M.; Yang, D.; Deng, Y.; Chen, P.; Zhou, H.; Qiu, X. Influence of pH on the behavior of lignosulfonate macromolecules in aqueous solution. *Colloids Surf., A* **2010**, *371*, 50−58.

(13) Qian, Y.; Deng, Y.; Qiu, X.; Huang, J.; Yang, D. Aggregation of sodium lignosulfonate above a critical temperature. *Holzforschung* **2014**, *68*, 641−647.
(14) Myrvold, B. O. Salting-out and salting-in experiments with lignosulfonates (LSs). *Holzforschung* **2013**, *67*, 549−557.
(15) Deng, Y.; Wu, Y.; Qian, Y.; Ouyang, X.; Yang, D.; Qiu, X. Adsorption and desorption behaviors of lignosulfonate during the self-assembly of multilayers. *BioResources* **2010**, *5*, 1178−1196.
(16) Myrvold, B. O. The Hansen solubility parameters of some lignosulfonates. *Int. J. Energy Power Eng.* **2015**, *9*, 261−264.
(17) Zulfikar, M. A.; Wahyuningrum, D.; Lestari, S. Adsorption of Lignosulfonate Compound from Aqueous Solution onto Chitosan-Silica Beads. *Sep. Sci. Technol.* **2013**, *48*, 1391−1401.
(18) Bai, B.; Grigg, R. B. Kinetics and Equilibria of Calcium Lignosulfonate Adsorption and Desorption onto Limestone. In *SPE International Symposium on Oilfield Chemistry*; Society of Petroleum Engineers: The Woodlands, Texas, 2005; p 11.
(19) Pang, Y.-X.; Qiu, X.-Q.; Yang, D.-J.; Lou, H.-M. Influence of oxidation, hydroxymethylation and sulfomethylation on the physicochemical properties of calcium lignosulfonate. *Colloids Surf., A* **2008**, *312*, 154−159.
(20) Ratinac, K. R.; Standard, O. C.; Bryant, P. J. Lignosulfonate adsorption on and stabilization of lead zirconate titanate in aqueous suspension. *J. Colloid Interface Sci.* **2004**, *273*, 442−454.
(21) Qiu, X.; Yan, M.; Yang, D.; Pang, Y.; Deng, Y. Effect of straight-chain alcohols on the physicochemical properties of calcium lignosulfonate. *J. Colloid Interface Sci.* **2009**, *338*, 151−155.
(22) Deng, Y.; Zhang, W.; Wu, Y.; Yu, H.; Qiu, X. Effect of Molecular Weight on the Adsorption Characteristics of Lignosulfonates. *J. Phys. Chem. B* **2011**, *115*, 14866−14873.
(23) Ouyang, X.; Deng, Y.; Qian, Y.; Zhang, P.; Qiu, X. Adsorption Characteristics of Lignosulfonates in Salt-Free and Salt-Added Aqueous Solutions. *Biomacromolecules* **2011**, *12*, 3313−3320.
(24) Zaki, N. N.; Ahmed, N. S.; Nassar, A. M. Sodium Lignin Sulfonate To Stabilize Heavy Crude Oil-In-Water Emulsions For Pipeline Transportation. *Pet. Sci. Technol.* **2000**, *18*, 1175−1193.
(25) Gundersen, S.; Ese, M.-H.; Sjöblom, J. Langmuir surface and interface films of lignosulfonates and Kraft lignins in the presence of electrolyte and asphaltenes: correlation to emulsion stability. *Colloids Surf., A* **2001**, *182*, 199−218.
(26) Zhang, T.; Ding, M.; Tao, N.; Wang, X.; Zhong, J. Effects of surfactant type and preparation pH on the droplets and emulsion forms of fish oil-loaded gelatin/surfactant-stabilized emulsions. *LWT−Food Sci. Technol.* **2020**, *117*, 108654.
(27) Aaen, R.; Brodin, F.; Simon, S.; Heggset, E.; Syverud, K. Oil-in-Water emulsions stabilized by cellulose nanofibrils—The effects of ionic strength and pH. *Nanomaterials* **2019**, *9*, 259.
(28) Hjartnes, T. N.; Sørland, G. H.; Simon, S.; Sjöblom, J. Demulsification of Crude Oil Emulsions Tracked by Pulsed Field Gradient (PFG) Nuclear Magnetic Resonance (NMR). Part I: Chemical Demulsification. *Ind. Eng. Chem. Res.* **2019**, *58*, 2310−2323.
(29) Lin, F.; Pang, C. J. Impact of a hybrid bitumen extraction process on the destabilization of resulting bitumen froth emulsion diluted with heptane. *Miner. Eng.* **2020**, *145*, 106069.
(30) Gundersen, S. A.; Sjöblom, J. High- and low-molecular-weight lignosulfonates and Kraft lignins as oil/water-emulsion stabilizers studied by means of electrical conductivity. *Colloid Polym. Sci.* **1999**, *277*, 462−468.
(31) Askvik, K. M. Complexation of lignosulfonates with multivalent cations and cationic surfactants, and the impact on emulsion stability. Ph.D. Thesis, University of Bergen, 2000.
(32) Gundersen, S. A. Lignosulfonates and Kraft lignins as oil-in-water emulsion stabilizers. Ph.D. Thesis, University of Bergen, 2000.
(33) Manasrah, K.; Neale, G.; Hornof, V. Properties of mixed surfactant solutions containing petroleum sulfonates and lignosulfonates. *Cellul. Chem. Technol.* **1985**, *19*, 291−299.
(34) D, R.; G, N.; V, H. Surface tension of mixed surfactant systems: lignosulfonate and sodium dodecyl sulfate. *Colloid Polym. Sci.* **2002**, *280*, 775−778.
(35) Askvik, K. M.; Are Gundersen, S.; Sjöblom, J.; Merta, J.; Stenius, P. Complexation between lignosulfonates and cationic surfactants and its influence on emulsion and foam stability. *Colloids Surf., A* **1999**, *159*, 89−101.
(36) Lebo, S. E.; Bråten, S. M.; Fredheim, G. E.; Lutnaes, B. F.; Lauten, R. A.; Myrvold, B. O.; McNally, T. J. Recent Advances in the Characterization of Lignosulfonates. In *Characterization of Lignocellulosic Materials*; Hu, T. Q., Ed.; Blackwell Publishing Ltd, 2008.
(37) Ralph, J.; Marita, J. M.; Ralph, S. A.; Hatfield, R. D.; Lu, F.; Ede, R. M.; Peng, J.; Landucci, L. L. Solution state NMR of lignins. In *Advances in Lignocellulosics Characterization*; TAPPI Press: Atlanta, 1999; pp 55−108.
(38) Ekeberg, D.; Gretland, K. S.; Gustafsson, J.; Bråten, S. M.; Fredheim, G. E. Characterisation of lignosulphonates and kraft lignin by hydrophobic interaction chromatography. *Anal. Chim. Acta* **2006**, *565*, 121−128.
(39) Israelachvili, J. *Intermolecular and Surface Forces*, 3rd ed.; Academic Press: Burlington, 2011.
(40) Tang, Q.; Zhou, M.; Li, Y.; Qiu, X.; Yang, D. Formation of Uniform Colloidal Spheres Based on Lignosulfonate, a Renewable Biomass Resource Recovered from Pulping Spent Liquor. *ACS Sustainable Chem. Eng.* **2018**, *6*, 1379−1386.
(41) Syahputra, A. E.; Tsau, J.-S.; Grigg, R. B. Laboratory Evaluation of Using Lignosulfonate and Surfactant Mixture in CO2 Flooding. In *SPE/DOE Improved Oil Recovery Symposium*; Society of Petroleum Engineers: Tulsa, Oklahoma, 2000.
(42) Tadros, T. F. *Emulsion Formation and Stability*; Wiley, 2013.
(43) Keleşoğlu, S.; Barrabino Ponce, A.; Humborstad Sørland, G.; Simon, S.; Paso, K.; Sjöblom, J. Rheological properties of highly concentrated dense packed layer emulsions (w/o) stabilized by asphaltene. *J. Pet. Sci. Eng.* **2015**, *126*, 1−10.
(44) Gundersen, S. A.; Sæther, Ø.; Sjöblom, J. Salt effects on lignosulfonate and Kraft lignin stabilized O/W-emulsions studied by means of electrical conductivity and video-enhanced microscopy. *Colloids Surf., A* **2001**, *186*, 141−153.

https://dx.doi.org/10.1021/acsomega.0c00616
ACS Omega 2020, 5, 15007−15015